Evaluation of the ECHAM family radiation codes performance in the representation of the solar signal

T. Sukhodolov[1,2], E. Rozanov[1,2], A.I. Shapiro[1], J. Anet[2], C. Cagnazzo[3], T. Peter[2], W. Schmutz[1]

[1]{Physical-Meteorological Observatory/World Radiation Center, Davos, Switzerland}

[2]{Institute for Atmospheric and Climate Science, ETH Zurich, Zurich, Switzerland}

[3]{Institute of Atmospheric Sciences and Climate of the Italian National Research Council, Rome, Italy}

Correspondence to: T. Sukhodolov (timofei.sukhodolov@pmodwrc.ch)

Abstract

Solar radiation is the main source of energy for the Earth's atmosphere and in many respects defines its composition, photochemistry, temperature profile and dynamics. The magnitude of the solar irradiance variability strongly depends on the wavelength making difficult its representation in climate models. Due to some deficiencies of the applied radiation codes several models fail to show a clear response in middle stratospheric heating rates to solar spectral irradiance variability, therefore it is important to prove a reasonable model performance in this respect before doing multiple model runs. In this work we evaluate the performance of three generations of ECHAM (4, 5 and 6) radiation schemes by comparison with the reference high resolution libRadtran code. We found that all original ECHAM solar radiation codes miss almost all solar signal in the heating rates in the mesosphere. In the stratosphere the 2-band ECHAM4 code (E4) has an almost negligible radiative response to solar irradiance changes, the 6-band ECHAM5 code (E5c) reproduces only about a half of the reference signal, while representation in the ECHAM6 code (E6) is better – it maximally misses about 15% in the upper stratosphere. On the basis of the comparison results we suggest necessary improvements of the ECHAM family codes by inclusion of available parameterizations of the heating rate due to absorption by oxygen (O_2) and ozone (O_3). Improvement is presented for E5c and E6, and both codes with the introduced

parameterizations represent the heating rate response to the spectral solar irradiance variability simulated with libRadtran much better without substantial increase of computer time. The suggested parameterizations are recommended to apply in the middle atmosphere version of the ECHAM-5 and 6 models for the study of the solar irradiance influence on climate.

1. Introduction

Although solar ultraviolet radiation (SUV) comprises only a couple of percent of the total solar irradiance (TSI), it plays a crucial role, largely defining the structure of the middle atmosphere. While the radiation in the visible (VIS) and infrared spectral ranges of the solar spectrum propagates through the atmosphere without significant absorption, almost all solar ultraviolet irradiance below 300 nm is absorbed by ozone and oxygen above the troposphere and represents the main source of energy in these regions. Furthermore, the SUV is strongly modulated by the solar rotational and 11-year solar cycles. Whereas the variability of TSI during 11 year solar activity cycle is around 0.1%, SUV variations can be more than 10 times higher. Moreover, recent measurements by the SORCE (SOLar Radiation and Climate Experiment) suggest a SUV variability significantly higher than all previous estimates (Ermolli et al., 2013 and references therein).

Changes in SUV irradiance lead to significant ozone, temperature, and zonal wind responses in the stratosphere and mesosphere, which has been shown in many modeling and observation data analysis studies (Hood and Soukharev, 2012; Austin et al., 2008; Gray et al., 2010; Haigh et al., 2010; Shapiro et al., 2013). The SUV is not considered as a direct radiative forcing for troposphere and surface, since it does not reach these altitudes, but there are indirect effects of solar irradiance variability, which are communicated downward in the so-called “top-down” mechanism: the modulation of stratospheric temperatures leads to dynamical feedbacks by affecting the Brewer-Dobson circulation and hence the stratosphere-troposphere exchange, resulting in decadal climate changes in the lower atmosphere (Solomon et al. 2007; Gray et al., 2010; Ermolli et al. 2013).

A comprehensive study of the entangled possible effects of solar variability requires chemistry-climate models (CCMs), the main instruments which are capable to take into account many atmospheric chemical, dynamical and temperature feedbacks. To this end, CCMs should contain a correct representation of the radiative transfer in the atmosphere.

Accurate codes for radiative transfer solution exist, e.g. LibRadtran (Mayer and Kylling, 2005), but they are too computationally expensive to be commonly used in global models. Therefore, different parameterizations have been designed to provide a compromise between accuracy and efficiency. Since most CCMs arise from global circulation models (GCMs), which are primarily tropospheric models, their radiation schemes carefully treat the longwave part of the spectrum, whereas the representation of the solar irradiance is coarse, approximating the entire UV/VIS spectral range by 1 or 2 spectral bands and not considering wavelengths shorter then ~250 nm. The evaluation of the radiation codes performed in the framework of the SPARC CCMVal-2 project (Forster et al., 2011, SPARC CCMval, 2010) have shown that only a few CCM radiation codes are capable of reproducing the magnitude and vertical profile of heating rate differences between solar minimum and maximum, which in turn directly depends on the treatment of the spectral resolution in the codes.

As was pointed out by Forster et al. (2011), a good representation of the solar signal can be obtained by increasing the number of spectral intervals. However, such an approach implies an increase of computational costs, which is a sensitive issue for already numerically expensive global CCMs (Nissen et al., 2007, Kubin et al., 2011). Nissen et al. (2007) has extended the 4-band scheme of Fouquart and Bonnel (1980) at model levels where the pressure is less than 70 hPa by a 49-band parameterization FUBrad and found out that the reduction of the FUBrad resolution to 6 bands results in a 20% loss of the solar variability induced changes in heating rates. There was no information about the differences in the CPU time taken by the parameterizations, however it is clear that this difference should be sufficiently higher than 20%, since the resolution was decreased by roughly 8 times. Another way is to apply parameterisations for the missed extra heating due to solar UV enhancement based on Beer-Lambert law (Strobel, 1978; Nicolet, 1985; Zhu, 1994). This method has been already used in MAECHAM-4 (Egorova et al., 2004) and CMAM (Fomichev et al., 2004) in order to parameterize the solar signal in missing and/or underrepresented spectral intervals and demonstrated good accuracy combined with very good efficiency. The most recent way to obtain satisfying results even with a relatively small number of spectral intervals is to use a completely different approach of incorporating non-gray gaseous absorption based on the so-called "correlated k-distribution" method (e.g. Fu and Liou, 1992). This method exploits the cumulative probability of the absorption coefficient in a spectral interval to replace wavenumber as an independent variable. Such a code is a part of ECHAM6, but its performance in respect to solar UV influence has not been checked which limits its application for solar-climate studies.

In this paper we evaluate the performance of the ECHAM family radiation codes in reproducing the heating rate response to SUV variability through the detailed comparison with the reference libRadtran code. We demonstrate the weaknesses of the ECHAM family solar radiation codes and suggest possible ways to improve their performance.

2. Description of the original ECHAM solar radiation codes

ECHAM is a family of atmospheric general circulation models developed by the Max Planck Institute for Meteorology (MPI-M) in Hamburg, Germany. The original ECHAM model branched from an early release of the ECMWF (European Center for Medium Range Weather Forecasts) model to enable climate studies (Simmons et al., 1989). It covered only the lower part of the atmosphere up to the 25-hPa level. Therefore, its solar radiation scheme (Fouquart and Bonnel, 1980) inherited by ECHAM was quite crude with respect to the shortwave part of spectrum, namely it had only one band covering the UV/VIS parts of the solar spectrum (250-680 nm) and one band covering near infrared (NIR), considered only absorption by O_3 and used TSI as input, i.e. change of the TSI was equally distributed among all spectral bands, and high shortwave variability was missed. This scheme (E4 hereafter) had been used up to ECHAM4 until the NIR part of this scheme was extended to 3 bands (Table 1) in ECHAM5 (E5 hereafter). The weakness of both this versions in representing the solar signal was demonstrated several times in stand-alone form (Solomon et al., 2007; Forster et al., 2011) and within CCMs (Egorova et al, 2004; Cagnazzo et al., 2007; Nissen et al., 2007): basically it has an almost negligible radiative response to solar irradiance changes due to the lack of wavelength dependence within the one broad UV/VIS band. Further E5 was also upgraded by Cagnazzo et al. (2007) by extending the number of spectral intervals from 1 in UV/VIS to 3 with 2 covering the UV range and switching to spectral solar irradiance (SSI) as input (E5c hereafter). This allowed reproducing about half of the reference heating rate differences (Forster et al., 2011). However, this scheme still does not contain any O_2 absorption.

One of the main improvements of ECHAM6 compared to previous versions was the adaptation of another solar radiation scheme, namely the Rapid Radiation Transfer model optimized for general circulation modeling studies (E6 hereafter) (Stevens et al., 2013). This scheme is ~10 times faster than previous schemes, it uses the correlated k-distribution method, and solar irradiance is calculated over a prescribed number of pseudo wavelength or g-points regarding to the absorbing features of certain wavelengths. Quadrature is performed over 112 g-points in the shortwave part of the spectrum, which then are grouped to 14 bands with 3 bands in UV (Table 1). The model has three UV spectral bands and considers oxygen absorption. However, the lowest wavelength boundary is 200 nm (Iacono et al., 2008), so that important features such as the solar Lyman-α (121.6 nm) line (LYA) and part of the Schumann- Runge oxygen absorption bands (SRB) are not taken into account.

3. Validation

To demonstrate the capabilities of the original codes we performed calculations with stand-alone versions of E4, E5c and E6 for the tropical standard atmosphere, with solar zenith angle equal to 10° and for solar minimum and maximum conditions. We have not analysed E5 separately since it has the same single UV/VIS band as E4. To validate the original schemes we compare all our calculations to the reference code LibRadtran (Mayer and Kylling, 2005), which has shown high accuracy in a number of intercomparison studies. For the 120-440 nm range LibRadtran considers more than 16000 wavelengths resolving in detail all relevant spectral features. Figure 1 shows the input information that we used to simulate solar variability: the solar irradiance changes, i.e. the relative difference between the irradiances during solar maximum and minimum conditions, and resulting solar-induced ozone changes. The irradiance spectrum for solar minimum and maximum conditions was calculated with Code for Solar Irradiance (Shapiro et al. 2010) following the approach presented in Shapiro et al. (2011). The solar minimum and maximum conditions correspond to sunspot numbers equal 0 and 120 respectively. We note that the spectral profile of the solar irradiance variability on the 11-year time scale yielded by the approach presented in Shapiro et al. (2011) agrees well with other reconstructions (Ermolli et al., 2013). Figure 1 shows that the solar irradiance variability is a very sophisticated function of wavelength. Resulting ozone changes were estimated from a composite of observational data (Soukharev and Hood, 2006; Austin et al. 2008; SPARC CCMVal, 2010).

Figure 2 illustrates the heating rates calculated by original E4, E5c and E6 schemes and by LibRadtran for solar maximum conditions and heating rate differences between solar maximum and minimum caused only by the solar irradiance changes. In terms of absolute values E5c and E6 underestimate heating rates compared to LibRadtran up to 2 and 3.5 Kday^{-}

$^{-1}$ correspondingly. This underestimation arises from 250–440 nm (E5) and 263–345 nm (E6) models bands i.e. from Hartley (HAR) and Huggins (HUG) ozone absorption bands. E4 (yellow line) shows underestimation instead, which is consistent with Cagnazzo et al. (2007) with respect to E5c. Cagnazzo et al. (2007) used another line-by-line model that was more consistent with E5c in the upper stratosphere, what means that found overestimation regarding to LibRadtran is comparable to the uncertainty range between line-by-line models. In the mesosphere E4 and E5c underestimate absolute values up to 5 and 7 Kday^{-1} since they do not take into account any oxygen absorption. E6 considers absorption by oxygen and shows adequate absolute values in the mesosphere.

In terms of heating rates response to SUV changes all schemes highly underestimate the solar signal in the mesosphere. At these altitudes heating rates are significantly defined by oxygen absorption in a highly variable LYA and SRB, which is completely missed in E4 and E5c and only slightly covered in E6. In the upper stratosphere E5c and E6 first bands covering Herzberg continuum and part of HAR are reproduced well. However, contribution from the second bands containing HAR and HUG is noticeably underestimated causing the main deviation from the reference model resulted in a total maximum 45 and 15 % deviation at 49 km for E5c and E6 correspondingly. E4 is able to reproduce only 7.5% of the signal at 49 km. Results of E4 and E5c are in agreement with previous comparison studies (Forster et al., 2011, SPARC CCMval, 2010). Underestimation of all schemes in HAR-HUG bands can be explained by a high spectral inhomogeneity of the solar irradiance variability in these regions (see Fig. 1), which is smoothed in integrated fluxes. Since the main disagreement appears in this wavelength region, it should be paid by more attention in the future evolution of heating rate parameterizations. In case if higher UV variability suggested by SORCE (Ermolli et al., 2013) is correct, the absolute values of the missed solar signal in heating rates would be respectively higher, providing more discrepancy to all feedbacks related to solar irradiance changes.

4. Implementation of the parameterizations

We do not consider E4 further, because its upgraded version was already discussed in Egorova et al (2004) and Forster et al. (2011) and currently it is not so widely used anymore as E5c and E6. To improve the representation of the solar signal we have implemented the parameterizations of the heating rates in the spectral regions, where we have found problems in the previous section. All parameterizations use the same approach based on Strobel (1978), deriving heating rates H from the atmosphere transmissivity of O_2 and O_3, using integrated fluxes of the solar radiation F as well as the ozone and oxygen number ($[O_2], [O_3]$) and column (N_2, N_3) density. For LYA we used the parameterization of Nicolet (1985)

$$H_{lya} = [O_2]\sigma_{lya}F_{lya}T_{o_2,lya}, \quad (1)$$

where the mean LYA absorption cross-section $\sigma_{lya} = 1.725 \times 10^{-18}/N_2^{0.1175}$ cm^2 and transmissivity $T_{o_2,\,lya} = \exp\left(-2.115\times 10^{18} N_2^{0.8855}\right)$.

From Zhu (1994) we used for SRB

$$H_{srb} = \frac{[O_2]x_{srb}F_{srb}}{\left(1+\frac{4\sigma_{srb}}{\pi y_{srb}}N_2\right)^{\frac{1}{2}}} \exp\left\{-\frac{\pi y_{srb}}{2}\left[\left(\left(1+\frac{4\sigma_{srb}}{\pi y_{srb}}N_2\right)^{\frac{1}{2}}\right)-1\right]\right\}, \quad (2)$$

where $\sigma_{srb} = 2.07 \times 10^{-24}$ m^2, $x_{srb} = \left(N_{2,top}/N_2\right)^{0.3}\sigma_{srb}$ and $y_{srb} = 0.0152$.

And for HAR and HUG we used

$$H_{har} = [O_3]\sigma_{har}F_{har}\exp(-\sigma_{har}N_3), \quad (3)$$

$$H_{hug} = \frac{[O_3]}{MN_3}\left\{F_{1,hug} + \left(F_{2,hug} - F_{1,hug}\right)\right\}exp\left(-\sigma_{hug}N_3 exp\left(-M\lambda_{long}\right) - F_{2,hug}exp\left(-\sigma_{hug}N_3 exp\left(-M\lambda_{short}\right)\right)\right), \quad (4)$$

where $M = 0.01273$ Å^{-1}, $\left(\lambda_{short}, \lambda_{long}\right) = (2805, 3015)$ Å, $\left(\sigma_{har}, \sigma_{hug}\right) = (8.7 \times 10^{-22}, 1.15 \times 10^{-6})$ m^2 and $F_{1,hug}$ and $F_{2,hug}$ are the integrated solar fluxes in the 280.5-305.5 and 305.5-360 nm ranges.

First, we have performed separate tests of these parameterizations which have shown that the parameterizations for HAR and HUG are in a good agreement with libRadtran. However, for LYA and SRB according to the test results we have changed σ_{lya} and added altitude dependent x_{srb}. Results of these tests are presented in Fig. 3. Then, since we use parameterizations to restore only a part of the heating rates variability, we have calculated scaling coefficients for each of the applied parameterizations separately for E5c and E6 (table 2) and implemented them to the original ECHAM codes. Since E5c does not have original absorption by oxygen and therefore underestimates the absolute values in the mesosphere, the heating parameterizations for LYA and SRB have been added to the original scheme using the full flux integrated within specific band in order to improve the scheme in respect to the calculation of the absolute heating rates. However to avoid an overestimation in the upper stratosphere, related to the fact that the original codes partially treat O_3 absorption in the Hartley and Huggins bands, we recommend to use not the full flux, but the difference between solar minimum and maximum. The same should be done for LYA and SRB in E6 to avoid an overestimation in the mesosphere, since the absolute values in the mesosphere are already reproduced well. In global models this can be done choosing the year with the lowest SSI in which all extra heating will be equal to zero, and then for calculations in all other years one should use the SSI difference from this "grand minimum" year.

4.1 Changing UV

Figure 4 shows the improvement of the original schemes performance due to the implemented parameterizations of O_2 and O_3 absorption calculated under changing UV and constant ozone conditions for tropical standard atmosphere and solar zenith angle equal to 10°. The implemented parameterizations of O_2 absorption allowed us to get very good agreement in solar variability induced heating rate changes with the reference model in the mesosphere, while the implemented parameterizations of O_3 absorption resulted in a very good agreement in the stratosphere. These parameterizations take negligible computer time compared to the time taken by radiation schemes and another advantage is that the inclusion of these parameterizations does not introduce any additional deviation to the absolute values of the heating rates compared to LibRadtran but only makes the difference between LibRadtran and E5c and E6 constant in time. The mean difference over the whole modelling time will be greater with extra heating than without extra heating, however the second one is less only because of the bad representation of the solar signal, and the first one will be equal to the difference in the "grand minimum" and will be constant in time. Therefore implementation of the proposed parameterizations does not require any retuning of the original codes.

Results of calculations with 4 other different atmosphere models (midlatitude summer, midlatitude winter, subarctic summer, subarctic winter (McClatchey et. al., 1972)) and 3 solar zenith angles (10°, 40°, 70°) presented in Fig. 5 have shown that the parameterizations work good for all conditions, and the applied scaling coefficients do not strongly depend on the position of the Sun and latitude and can be used in models with high confidence. It should be noted that for other radiation schemes and other SSI data sets these coefficients will differ and have to be carefully calculated regarding to the specific features of each scheme.

4.2 Changing ozone.

For the previous calculations we have used only changing UV fluxes with a constant ozone profile, but ozone profile is modulated by solar irradiance changes and these two features are closely related. To check the parameterization applicability taking into account the ozone feedback we have also calculated the heating rate response to the solar induced ozone changes keeping the UV fluxes unchanged. Results of these calculations are shown in Fig. 6. In this case the original codes work well, and since we use irradiance differences to calculate extra heating, we do not affect heating rates by ozone changes, because extra-heating rates in this case are equal to zero. The total heating rate (UV + ozone) also looks good compared to the reference model.

5. Conclusions

We have evaluated the performance of the ECHAM4, 6-band ECHAM5 and ECHAM6 radiation codes in the representation of the solar UV variability induced changes in the heating rates. All schemes have shown high underestimation in the mesosphere. In the stratosphere ECHAM4 code is able to reproduce only 7.5% of the reference solar signal, while 6-band ECHAM5 code misses 45% and ECHAM6 code misses about 15%. We suggested an accurate method to correct the revealed problems by the implementation of parameterizations of extra heating due to oxygen and ozone absorption. This approach was implemented to the 6-band ECHAM5 and ECHAM6 schemes and allowed us to get very good agreement with the reference model in the representation of the solar signal in the mesosphere and stratosphere without significant increase of computational time. This method does not require tuning of the original codes, but it only provides the solar induced addition to original heating rates. Therefore this method is suitable for any other radiation scheme to correct the solar signal in heating rates due to missing or underrepresented spectral intervals. It should be noted that the coefficients of the parameterizations should be re-evaluated regarding to the features of any particular scheme.

Acknowledgments

This research was funded in part by the Swiss National Science Foundation under grant agreements 200020 140573, and CRSI122-130642 (FUPSOL). Fruitful discussions inside COST Action ES1005 TOSCA (http://www.tosca-cost.eu) community are much appreciated.

References

Austin, J., Tourpali, K., Rozanov, E., Akiyoshi, H., Bekki, S., Bodeker, G., Brühl, C., Butchart, N., Chipperfield, M., Deushi, M., Fomichev, V. I., Giorgetta, M. A., Gray, L., Kodera, K., Lott, F., Manzini, E., Marsh, D., Matthes, K., Nagashima, T., Shibata, K., Stolarski, R. S., Struthers, H., and Tian, W.: Coupled chemistry climate model simulations of the solar cycle in ozone and temperature, J. Geophys. Res.-Atmos., 113, D11306, doi:10.1029/2007JD009391, 2008.

Cagnazzo, C., Manzini, E., Giorgetta, M. A., Forster, P. M. D., and Morcrette, J. J.: Impact of an improved shortwave radiation scheme in the MAECHAM5 General Circulation Model, Atmos. Chem. Phys., 7(10), 2503–2515, doi:10.5194/acp-7-2503-2007, 2007.

Egorova, T., Rozanov, E., Manzini, E., Haberreiter, M., Schmutz, W., Zubov, V., and Peter, T.: Chemical and dynamical response to the 11-year variability of the solar irradiance simulated with a chemistry-climate model, Geophys. Res. Lett., 31, L06119, doi:10.1029/2003GL019294, 2004.

Ermolli I., Matthes, K., Dudok de Wit, T., Krivova, N. A., Tourpali, K., Weber, M., Unruh, Y. C., Gray, L., Langematz, U., Pilewskie, P., Rozanov, E., Schmutz, W., Shapiro, A., Solanki, S. K., and Woods, T. N.: Recent variability of the solar spectral irradiance and its impact on climate modelling, Atmos. Chem. Phys., 13, 3945–3977, 2013, doi:10.5194/acp-13-3945-2013, 2013.

Fomichev, V. I., C. Fu, J. de Grandpré, S. R. Beagley, V. P. Ogibalov, and J. C. McConnell, Model thermal response to minor radiative energy sources and sinks in the middle atmosphere, J. Geophys. Res., 109, D19107, doi:10.1029/2004JD004892, 2004.

Forster, P. M., Fomichev, V. I., Rozanov, E., Cagnazzo, C., Jonsson, A. I., Langematz, U., Fomin, B., Iacono, M. J., Mayer, B., Mlawer, E., Myhre, G., Portmann, R. W., Akiyoshi, H., Falaleeva, V., Gillett, N., Karpechko, A., Li, J., Lemennais, P., Morgenstern, O., Oberlander, S., Sigmond, M., and Shibata, K.: Evaluation of radiation scheme performance within chemistry climate models, J. Geophys. Res.- Atmos., 116, D10302, doi:10.1029/2010JD015361, 2011.

Fouquart, Y. and Bonnel, B.: Computations of solar heating of the earth's atmosphere - A new parameterization. Beitr. Phys. Atmosph., 53, 35-62, 1980.

Fu, Q. and Liou, K. N.: On the correlated k-distribution method for radiative transfer in nonhomogeneous atmospheres, J. Atmos. Sci., 49, 2139-2156, 1992.

Gray, L. J., Beer, J., Geller, M., Haigh, J. D., Lockwood, M., Matthes, K., Cubasch, U., Fleitmann, D., Harrison, G., Hood, L., Luterbacher, J., Meehl, G. A., Shindell, D., van Geel, B., and White, W.: Solar influences on climate, Rev. Geophys., 48, RG4001, doi:10.1029/2009RG000282, 2010.

Haigh, J. D., Winning, A. R., Toumi, R., and Harder, J.W.: An influence of solar spectral variations on radiative forcing of climate, Nature, 467, 696–699, doi:10.1038/nature09426, 2010.

Hood, L. L., Soukharev B. E.: The Lower-Stratospheric Response to 11-Yr Solar Forcing: Coupling to the Troposphere–Ocean Response. J. Atmos. Sci., 69, 1841–1864, 2012.

Iacono, M. J., Delamere, J. S., Mlawer, E. J., Shephard, M. W., Clough, S. A., and Collins, W. D.: Radiative forcing by long-lived greenhouse gases: Calculations with the AER radiative transfer models. J Geophys Res-Atmos, 113 (D13), 2008.

Kubin, A., Langematz, U., and Bruehl, C.: CCM simulations of the effect of the 27-day solar rotational cycle on ozone, J. Geophys. Res., 116, D15301, doi:10.1029/2011JD015665, 2011.

Mayer, B. and Kylling, A.: Technical Note: The libRadtran software package for radiative transfer calculations: Description and examples of use, Atmos. Chem. Phys., 5, 1855–1877, 2005, http://www.atmos-chem-phys.net/5/1855/2005/.

McClatchey, R. A., Fenn, R. W., Selby, J. E. A., Volz, F. E., and Garing, J.S.: Optical Properties of Atmosphere (Third Edition), AFCRL-72-0497, 1972.

Nicolet, M.: Aeronomical aspects of mesospheric photodissociation: Processes resulting from the solar H Lyman-alpha line, Planet. Space Sci., 33, 69–80, 1985.

Nissen, K. M., Matthes, K., Langematz, U., and Mayer, B.: Towards a better representation of the solar cycle in general circulation models, Atmos. Chem. Phys., 7, 5391–5400, doi:10.5194/acp-7-5391-2007, 2007.

Shapiro, A. V., Rozanov, E. V., Shapiro, A. I., Egorova, T. A., Harderi, J., Weber, M., Smith, A. K., Schmutz, W., and Peter, T.: The role of the solar irradiance variability in the evolution of the middle atmosphere during 2004–2009, J. Geophys. Res.-Atmos., doi:10.1002/jgrd.50208, 2013.

Shapiro, A. I., Schmutz, W., Rozanov, E., Schoell, M., Haberreiter, M., Shapiro, A. V., and Nyeki, S.: A new approach to the long-term reconstruction of the solar irradiance leads to large historical solar forcing, Astron. Astrophys., 529, A67, doi:10.1051/0004-6361/201016173, 2011.

Shapiro, A. I., Schmutz, W., Schoell, M., Haberreiter, M., and Rozanov, E.: NLTE solar irradiance modeling with the COSI code, Astron. Astrophys., 517, A48, doi:10.1051/0004-6361/200913987, 2010.

Simmons, A.J., Burridge, D.M., Jarraud, M., Girard, C., and Wergen, W.: The ECMWF medium-range prediction models: Development of the numerical formulations and the impact of increased resolution. Meteorol. Atmos. Phys., 40, 28-60, 1989.

Solomon, S. D., Qin, D., Manning, M., Chen, Z., Marquis, M., Averyt, K. B., Tignor, M., and Miller, H.: Climate Change 2007: The Physical Science Basis (Contribution of Working Group I to the Fourth Assessment Report of the Intergovernmental Panel on Climate Change), Cambridge Univeristy Press, Cambridge, UK, 2007.

Soukharev, B. E. and Hood, L. L.: Solar cycle variation of stratospheric ozone: Multiple regression analysis of long-term satellite data sets and comparisons with models, J. Geophys. Res., 111, D20314, doi:10.1029/2006JD007107, 2006.

SPARC CCMVal (2010), SPARC Report on the Evaluation of Chemistry-Climate Models, edited by V. Eyring, T. G. Shepherd, and D. W. Waugh, SPARC Rep. 5, Univ. of Toronto, Toronto, Ont., Canada. (Available at http://www.atmosp.physics.utoronto.ca/SPARC.)

Stevens, B., Giorgetta, M., Esch, M., Mauritsen, T., Crueger, T., Rast, S., Salzmann, M., Schmidt, H., Bader, J., Block, K., Brokopf, R., Fast, I., Kinne, S., Kornblueh, L., Lohmann, U., Pincus, R., Reichler, T., Roeckner, E.: Atmospheric component of the MPI-M Earth System Model: ECHAM6. J. Adv. Model. Earth Syst, 2013.

Strobel, D. F.: Parameterization of the atmospheric heating rate from 15 to 120 km due to O2 and O3 absorption of solar radiation, J. Geophys. Res., 83, 6225–6230, 1978.

Zhu, X.: An accurate and efficient radiation algorithm for middle atmosphere models, J. Atmos. Sci., 51, 3593–3614, 1994.

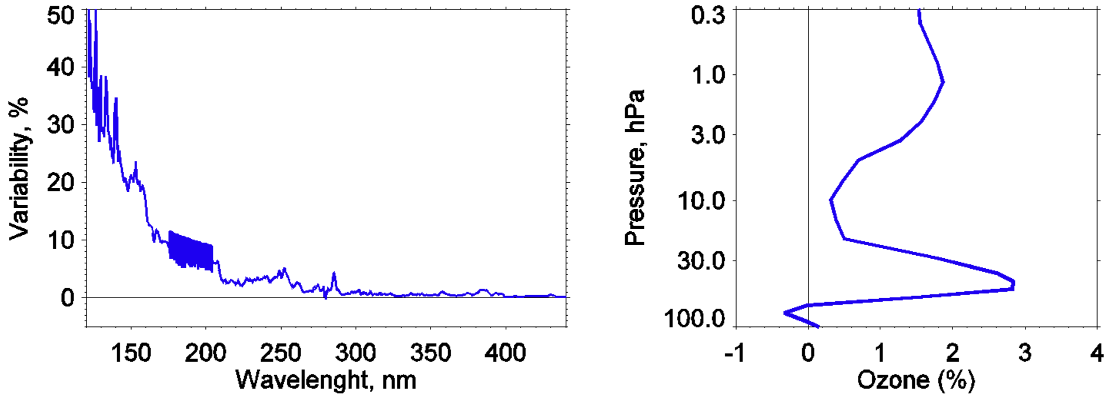

Fig. 1. Variability of solar irradiance in the 120-440 nm wavelength range calculated by COSI (left) and resulting ozone response from a composite of observational data from Soukharev and Hood (2006) and Austin et al. (2008) (right).

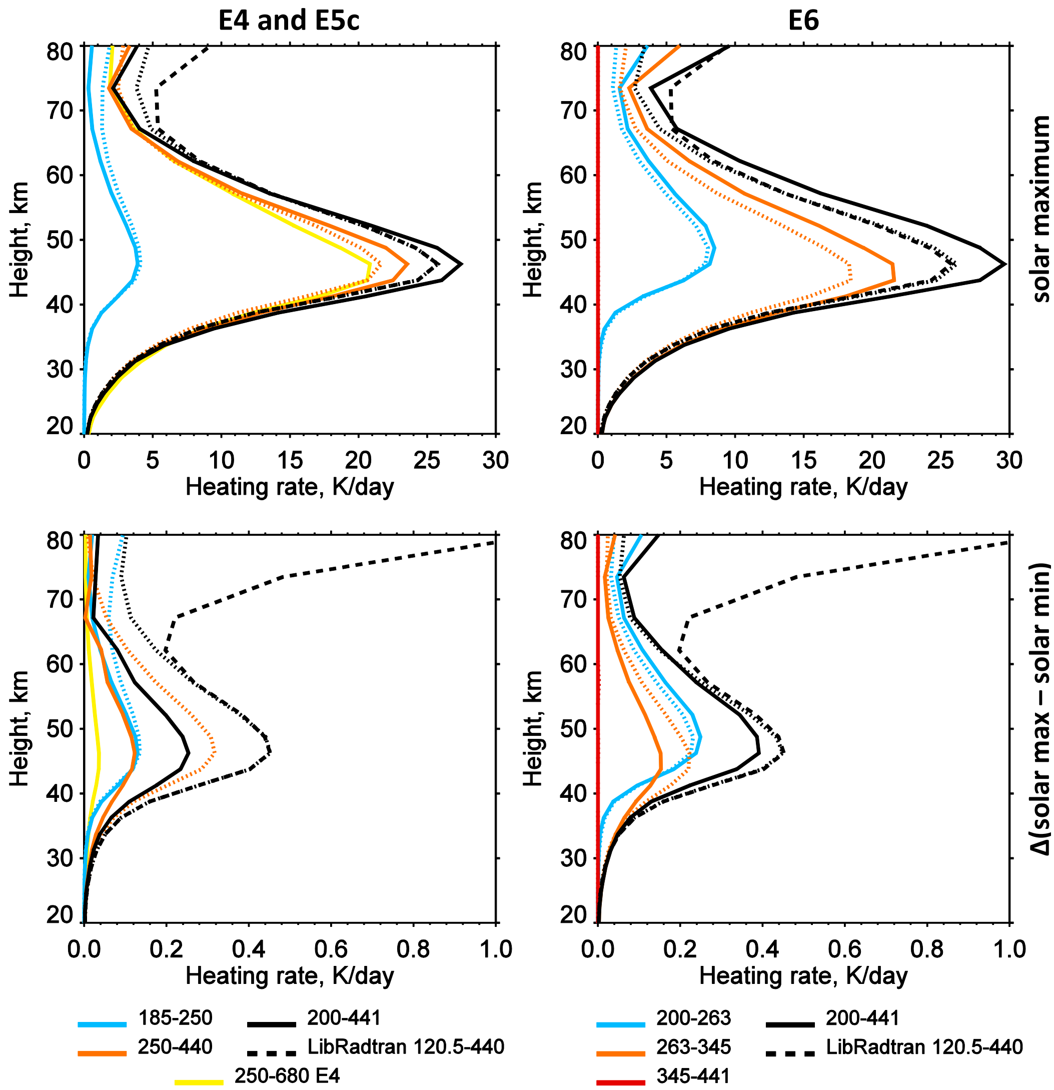

Fig. 2. Shortwave heating rates in Kday^{-1} for tropical standard atmosphere and solar zenith angle equal to 10° calculated by E5c nad E4 (left pictures) and E6 (right pictures). Top panels: absolute values during solar maximum. Bottom panels: differences between minimum and maximum (max-min) of the 11-year solar cycle. Solid lines: ECHAM results. Dotted lines: LibRadtran results for the same spectral intervals. Different spectral intervals are designated by colours, yellow line – E4 250–680 band. Black dashed line: LibRadtran results for 120-440 nm (i.e. including shortest wavelengths > 120 nm).

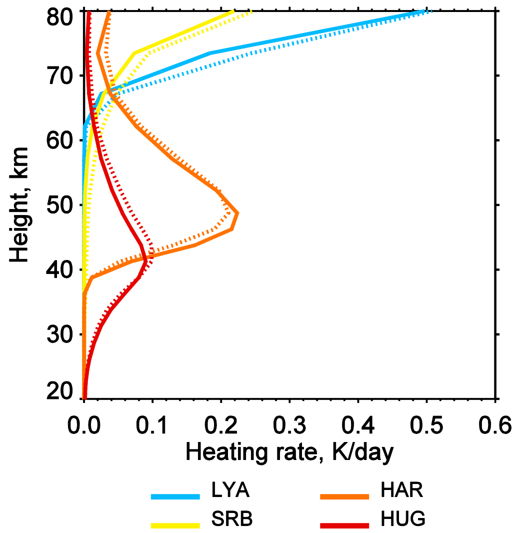

Fig. 3. Shortwave heating rate differences of the 11-year solar cycle (solar max minus solar min) in $K day^{-1}$ for tropical standard atmosphere and solar zenith angle equal to 10° calculated by extra heating parameterizations and LibRadtran. Solid lines: results of parameterizations. Dotted lines: LibRadtran results for the same spectral intervals (table 1).

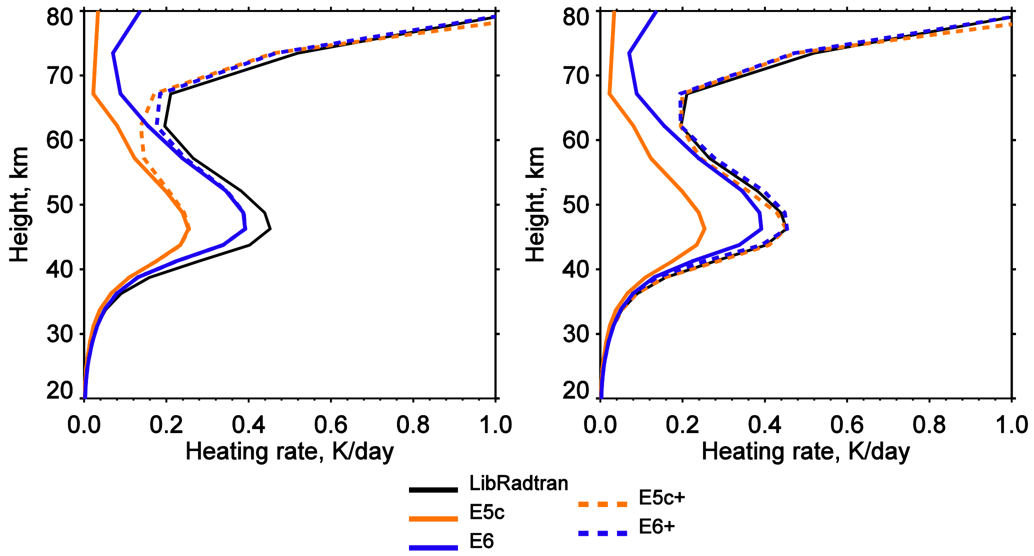

Fig. 4. Shortwave heating rate differences of the 11-year solar cycle (solar max minus solar min) in Kday^{-1} for tropical standard atmosphere and solar zenith angle equal to 10° in case of UV only variability and constant ozone profile. Coloured solid lines: results from original codes. Black solid line: LibRadtran results for reference. Dashed lines: results from improved parameterizations. Left panel: improvement due to implementation of O_2 absorption parameterization only. Right panel: O_2 and O_3 absorption parameterization.

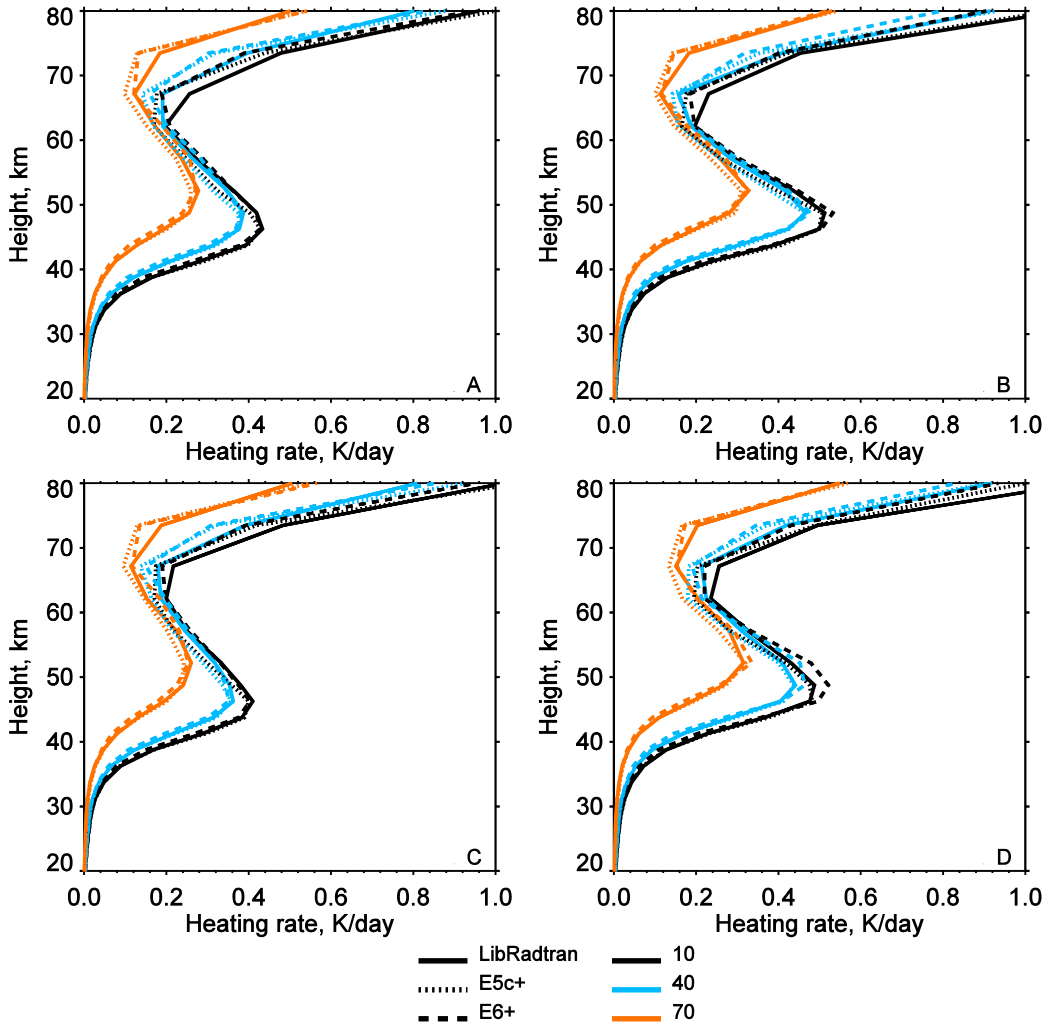

Fig. 5. Shortwave heating rate differences (solar max minus solar min) of the 11-year solar cycle in $K day^{-1}$ for 4 standard atmospheres: A - midlatitude summer, B - midlatitude winter, C - subarctic summer, D – subarctic winter. Solid lines: LibRadtran. Dashed lines: E6+ (E6 including corrections to 120 nm). Dotted lines: E5c+. Colours: different solar zenith angles (black 10°, blue 40°, orange 70°).

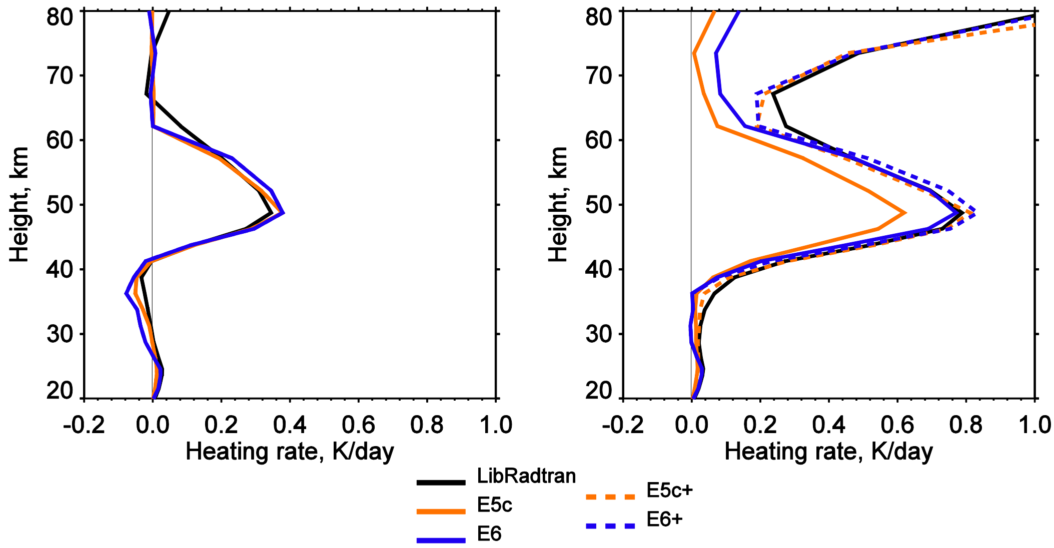

Fig. 6. Shortwave heating rate differences (solar max minus solar min) of the 11-year solar cycle in $K day^{-1}$ for tropical standard atmosphere and solar zenith angle equal to 10°. Left panel: including only ozone changes. Right panel: UV + ozone changes. Original codes results are denoted by solid lines, improved codes results – by dashed lines.

Table 1. ECHAM radiation schemes spectral intervals and main absorbers in the UV part of spectrum.

Scheme	E4	E5	E5c	E6	
Main absorbers in the UV	O_3	O_3	O_3	O_2, O_3	
Wavelength bands	250 – 680	185 – 250	185 – 250	200 – 263	1298 – 1626
	680 - 4000	690 – 1190	250 – 440	263 – 345	1626 – 1942
		1190 - 2380	440 - 690	345 – 441	1942 - 2151
		2380 - 4000	690 - 1190	441 – 625	2151 – 2500
			1190 - 2380	625 – 778	2500 – 3077
			2380 - 4000	778 – 1242	3077 – 3846
				1242 – 1298	3846 - 12195

Table 2. Wavelength intervals and scaling coefficients of the extra heating parameterizations.

Parameterization	Wavelength interval (nm)	Scaling coefficients	
		E5c	E6
LYA	121.0 – 122.0	0.5	1.2
SRB	175.0 – 205.0	3.5	1.0
HAR	250.0 – 280.0	0.7	0.25
HUG	280.5 – 360.0	0.3	0.0